Geophysical Research Letters

RESEARCH LETTER
10.1029/2022GL098780

Modeling Snow Dynamics and Stable Water Isotopes Across Mountain Landscapes

Rosemary W. H. Carroll[1], Jeffrey Deems[2], Matthias Sprenger[3], Reed Maxwell[4], Wendy Brown[5], Alexander Newman[5], Curtis Beutler[5], and Kenneth H. Williams[3,5]

[1]Desert Research Institute, Reno, NV, USA, [2]National Snow and Ice Data Center, Boulder, CO, USA, [3]Lawrence Berkeley National Laboratory, Berkeley, CA, USA, [4]Princeton University, Princeton, NJ, USA, [5]Rocky Mountain Biological Laboratory, Gothic, CO, USA

Key Points:

- Precipitation timing, phase, and isotopic value dominate meltwater inputs. Fractionation accounts for less than 25% total enrichment
- The most depleted isotopic water inputs occur in the upper subalpine where snow accumulation is high and rainfall is low
- Deep snowpack and shading of conifer forests limit the influence of vapor loss on snowmelt

Supporting Information:

Supporting Information may be found in the online version of this article.

Correspondence to:

R. W. H. Carroll,
rosemary.carroll@dri.edu

Citation:

Carroll, R. W. H., Deems, J., Sprenger, M., Maxwell, R., Brown, W., Newman, A., et al. (2022). Modeling snow dynamics and stable water isotopes across mountain landscapes. *Geophysical Research Letters*, *49*, e2022GL098780. https://doi.org/10.1029/2022GL098780

Received 21 MAR 2022
Accepted 3 OCT 2022

Author Contributions:

Conceptualization: Rosemary W. H. Carroll, Jeffrey Deems, Matthias Sprenger, Reed Maxwell
Data curation: Kenneth H. Williams
Formal analysis: Rosemary W. H. Carroll, Matthias Sprenger, Reed Maxwell, Alexander Newman
Funding acquisition: Kenneth H. Williams
Investigation: Jeffrey Deems, Wendy Brown, Alexander Newman, Curtis Beutler, Kenneth H. Williams
Methodology: Rosemary W. H. Carroll, Matthias Sprenger

Abstract A coupled hydrologic and snowpack stable water isotope model assesses controls on isotopic inputs across a mountainous basin. Annually, the most depleted isotope conditions occur in the upper subalpine where snow accumulation is high, and rainfall is low. Snowmelt isotopic evolution over time indicates fractionation processes account for <25% snowmelt enrichment. Meltwater isotopic inputs are largely determined by controls on the amount, phase and isotopic mass of precipitation coincident with the ablation period. Effect of vapor loss from the snowpack on d-excess in snowmelt is a balance between energy and snow-availability. It is highest above treeline, and in the grass and aspen-dominated portions of the upper montane where vegetation shading is low. Deep snowpack in conifer forests limit the influence of vapor loss in the subalpine. Wet years reduce the effects of vapor loss on snowmelt across the basin, except in the lower montane where added snowfall bolsters snow-limited conditions.

Plain Language Summary Stable water isotopes are used in hydrology to track vegetation water use and stream water source. Watersheds reliant on snow alter the timing of water inputs through snow storage and melt and may produce a different isotopic input signal due to evaporation of the snowpack prior to melt. We combine a hydrologic and snowpack isotope model to understand how landscape position and climate may affect isotopic water inputs in a large mountain basin with nearly 2 km in vertical relief. The lightest isotopes occur in the upper subalpine where snow accumulation is highest and rain inputs are low. The temporal evolution of isotopes in snowmelt is largely controlled by elevation and its influence on the amount, phase (rain or snow) and isotopic mass of spring precipitation coincident with the snowmelt period. Snowpack alterations account for <25% total snowmelt enrichment. Changes to the snowpack isotopic signature by vapor loss are most important where vegetation does not shade the snow, where moderate snowfall occurs and evaporation potential is relatively high. Changes are highest above treeline and in areas with meadows and aspen forests. Vapor loss effects on snowpack are lowest in the deep snow found in conifer forests, and in snow-limited lower elevations.

1. Introduction

Stable isotopes of water have long been used as tracers in hydrologic research to identify the partitioning of rain and snow to vegetation water use (Berkelhammer et al., 2020; Sprenger et al., 2016), groundwater recharge (Earman et al., 2006; Fiorella et al., 2018; Jasechko, 2019; Oiro et al., 2018), and stream water (Cowie et al., 2017; Zhang et al., 2018). Isotopic mass balance studies in watersheds reliant on snow water must adjust isotopic boundary influxes as a function of snow storage and snowmelt timing, and the potential for isotopic modification due to post-depositional fractionation in the snowpack. While isotopic fractionation processes in snow are well defined (Beria et al., 2018), less work has addressed these processes at watershed-scales in mountain environments. Challenges are largely due to obtaining hydrologic and isotopic observations at the scales important to snow processes (Bales et al., 2006; Clark et al., 2011; Mott et al., 2018). Temporal scales are defined by meteorological inputs needed to quantify the energy balance of the snowpack (≤daily), while the spatial resolution needed to capture non-uniform hydrologic processes in mountain systems is on the order of 100–250 m (Baba et al., 2019; Foster et al., 2020). An added complication arises given most of snow resides near treeline (Carroll et al., 2019) with regular and safe access for field samples often not possible. As a consequence, isotopic tracer studies in mountain environments tend to extrapolate limited plot-scale data across an entire watershed (Bearup

Project Administration: Kenneth H. Williams
Resources: Jeffrey Deems, Wendy Brown, Alexander Newman, Curtis Beutler, Kenneth H. Williams
Supervision: Kenneth H. Williams
Visualization: Rosemary W. H. Carroll, Reed Maxwell, Alexander Newman
Writing – original draft: Rosemary W. H. Carroll

et al., 2014; Carroll et al., 2018; Evans et al., 2016; Fang et al., 2019) with the potential to introduce significant error in water source estimates dependent on isotopic inputs.

With respect to time-variable isotopic inputs from snowmelt, these have largely been confined to laboratory experiments (Feng et al., 2002; Taylor, Feng, Renshaw, & Kirchner, 2002; Taylor, Feng, Williams, & McNamara, 2002) or to field studies focused on plot (Friedman et al., 1991; Stichler et al., 1981; Taylor et al., 2001) or hillslope scales (Evans et al., 2016). More recently, Ala-aho et al. (2017) incorporated changes in snow isotopic values with a snow process model to estimate a spatio-temporally distributed isotope signal into basins with contrasting snow conditions. We apply work by Ala-aho et al. (2017) across a much larger Colorado River headwater basin with greater relief and constrain the model using a comprehensive isotopic data set. With this data-modeling framework, we investigate water isotopic inputs at high spatial and temporal resolution over multiple years with reference to snow processes. Our objective is to isolate key controls on isotopic water inputs and better constrain the relative importance of fractionation on these inputs.

1.1. Stable Water Isotope Overview

Stable water isotopes are reported as the ratio of heavier to lighter isotope in a sample (R_{sample} = ^{18}O/^{16}O, or ^{2}H/^{1}H) relative to the Vienna Standard Mean Ocean Water standard (R_{VSMOW}). Results are presented in units of per mil (‰) as $\delta = 1000 * \left(R_{\text{sample}} - R_{\text{VSMOW}}\right) / R_{\text{VSMOW}}$. The second order isotope parameter, d-excess (d-excess = δ^2H-8δ^{18}O) expresses the deviation of local samples from the global meteoric water line (GMWL) as plotted in the dual-isotope space (δ^2H = 8δ^{18}O+10). D-excess decreases in response to kinetic processes resulting from the molecular mass differential between oxygen and hydrogen during vapor loss. Specifically, the lighter ^{2}H molecule turns to vapor more readily than the heavier ^{18}O molecule. A lowering of d-excess from its initial isotopic state indicates either evaporation or sublimation (Clark & Fritz, 1997). In this study, we define the initial state as the isotopic composition of net precipitation. After deposition, the ratios of heavy to light isotopes in the snowpack can vary due to diffusional transport of water from the soil, temperature-gradient induced vapor diffusion within the snow column, lateral flow through the snowpack and fractionation processes associated with sublimation, evaporation, and melt-freeze cycles (Beria et al., 2018; Cooper, 1998; Evans et al., 2016; Friedman et al., 1991; Sinclair & Marshall, 2008; Stichler et al., 1981).

2. Site Description and Modeling Strategy

The East River, Colorado (ER, 750 km^2) is a headwater basin of the Colorado River in the southwestern US with elevations ranging from 2,440 to 4,346 m. Climate for the area is continental subarctic. Average annual precipitation is 1,434 ± 258 mm/yr with 15 ± 7% falling as rain. Most rain occurs during the summer monsoon (Carroll et al., 2020). Water years considered in this study (2016–2020) overlap a comprehensive isotopic sampling campaign. Water year 2016 represents average snow conditions, and 2018 and 2019 represent dry/warm and wet/cool snow conditions, respectively. Ecozones are broadly defined by elevation and dominant vegetation cover (Figures 1a and 1c). Montane conditions (<2,800 m) contain shrubs, grasses and some aspen forest, with the lower montane differentiated by high aridity (potential evapotranspiration to precipitation, PET/P, Figure 1d). The lower subalpine contains conifer forests mixed with aspen (2,800–3,200 m) and the upper subalpine is a combination of lower density conifer forests, shrubs and barren ground (3,200–3,500 m). The alpine (>3,500 m) occurs above treeline. The transition from water-to energy-limited conditions (PET/P = 1) occurs at the interface between the lower and upper subalpine.

The hydrologic model was originally developed by Carroll et al. (2022). It uses the semi-empirical, spatially distributed U.S. Geological Survey (USGS) numerical code Precipitation Runoff Modeling System (PRMS, Markstrom et al., 2015). Water and energy are tracked daily through the atmosphere, canopy and subsurface at a 100 m grid resolution. Daily climate forcing assigns minimum and maximum temperature lapse rates based on two local snow-telemetry stations and is adjusted for aspect. The spatial distribution of snow water equivalent (SWE) follows previous work (Carroll et al., 2019, 2020) and is based on airborne light-detection and ranging (LiDAR) (Painter et al., 2016). The approach implicitly allows redistribution of snow by wind and avalanche to move snow off mountain ridges and into high elevation cirque valleys to produce the deepest snowpack near treeline. Precipitation phase (rain, snow) for a given location is controlled by a user-defined temperature

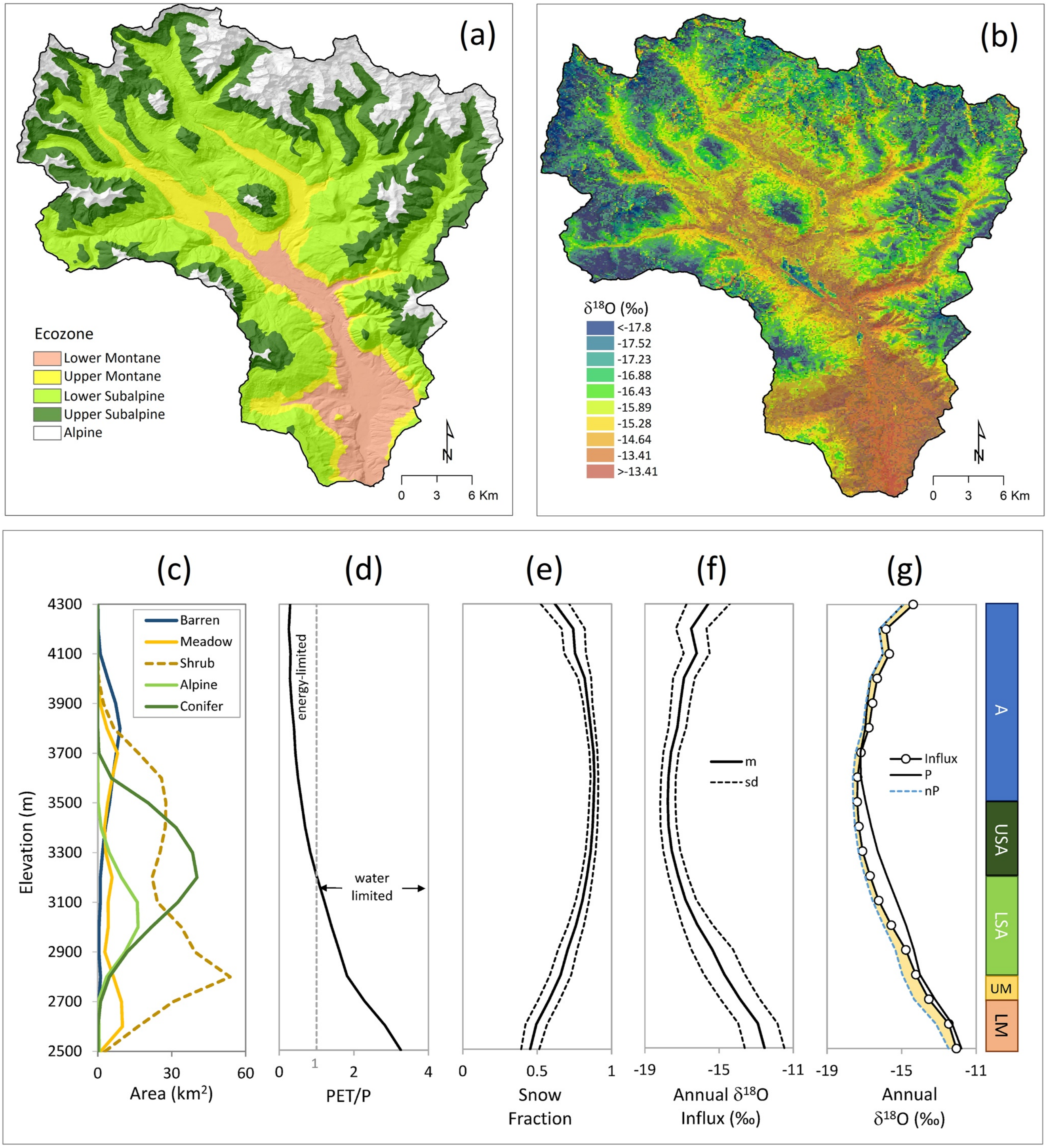

Figure 1. Simulated (a) ecozones, and (b) annual influx δ^{18}O for an average water year across the East River. Elevation averages for (c) cover type, (d) aridity or potential evapotranspiration to precipitation, PET/P, (e) snow fraction mean and standard deviation for years 2016–2020, (f) annual influx δ^{18}O mean and standard deviation for years 2016–2020, (f) isotopic distribution of δ^{18}O in precipitation, P, and net precipitation, nP, compared to $\delta\ ^{18}$O influx for an average water year. Yellow shaded area is enrichment due to fractionation processes. A = alpine, USA = upper subalpine, LSA = lower subalpine, UM = upper montane, LM = lower montane.

threshold. Precipitation contributes water to the snowpack and adds/subtracts energy content based on its phase and temperature. Shortwave radiation at the snowpack surface is limited by the winter vegetation transmission coefficient and reduced by the estimated albedo. Trees and shrubs are assumed to diminish wind, and the energy applied to the snowpack in these areas is reduced by half. Sublimation is calculated with a user-defined fraction of PET adjusted for heat deficit in the snowpack and snow-covered area. Canopy interception is simulated based on water holding capacity dependent on cover type and canopy density. Stored precipitation can only be lost back to the atmosphere through evaporation. Net precipitaton is the amount of precipitation that is not captured by the canopy and reaches the ground. Hydrologic model calibration matches mean monthly solar radiation, daily snow depth at four weather stations, and streamflow. Model verification is based on spatially distributed SWE from four LiDAR campaigns, SWE at individual snowpits, and eddy covariance flux estimates. While some details on the hydrologic model are given in the Supporting Information S1, please refer to Carroll et al. (2022) for a full description of model calibration and verification.

Snowpack samples for isotopic model constraint were collected years 2016–2020 from 81 snowpits spanning gradients in topography, vegetation and seasonal climate (Figure S1 in Supporting Information S1). Overlapping isotopic campaigns for precipitation and snowmelt were also conducted. Analysis of the data by Carroll et al. (2022) found observed snowfall $\delta^{18}O$ directly related to air temperature with a slope in the dual isotope space similar to the GMWL (slope = 8.2). D-excess in snowfall was directly related to temperature. Observed $\delta^{18}O$ in rainfall was dependent on air temperature and modified by wind speed. Rain was heavier than snowfall and fell below the GMWL (slope = 6.8). Rain d-excess had a lower value than snow and correlated to temperature and reltive humidity. The observed isotopic elevational lapse rate in precipitation was −0.16‰ $\delta^{18}O$ per 100-m and similar to other studies in North America (Friedman et al., 1992; Tappa et al., 2016). Annually, the mean isotopic inputs in snowfall describe the observed $\delta^{18}O$ mean in snowpack. In contrast, observed snowpack d-excess declined at low elevation and where solar radiation was high. The rate of observed snowmelt enrichment increased at lower elevations.

The isotope mass balance model follows Ala-aho et al. (2017) to track $\delta^{18}O$ entering the soil system as snowmelt or as rain when SWE = 0. The approach is expanded to include $\delta^{2}H$ and d-excess. Water stores and fluxes needed for the isotope model use hydrologic model output for each timestep and model grid location. Similar to Ala-aho et al. (2017), isotopic parameters related to fractionation are estimated using a Monte Carlo approach with uniform input distributions and 1,000 realizations. Modeled fit is based on a composite metric combining each isotope parameter ($\delta^{2}H$, $\delta^{18}O$, d-excess) and type of observation (SWE, snowmelt). The final parameter suite for melt, evaporative and kinetic fractionation is determined from the average of the 10-best realizations with the lowest composite rRMSE. The isotopic model calibration is done independent of the hydrologic model. A full description of the snowpack isotope model, evaluation metrics and calibration are provided in the SI and the associated data package.

3. Results

The spatial distribution of annual $\delta^{18}O$ terrestrial influxes for an average water year is given in Figure 1b. Results are also condensed to elevation. The most depleted values (−17.8 ± 0.4‰, Figure 1f) occur at the transition between the upper subalpine and alpine where the snow fraction (0.90 ± 0.04, Figure 1e) and spring snow water inputs are largest. Relatively heavier isotopes occur in the alpine (−15.6 ± 1.2‰) and montane (−12.5 ± 1.1‰). $\delta^{18}O$ influxes are slightly more enriched than net precipitation (+0.4 ± 0.2‰, Figure 1g yellow shading) with the largest average snowmelt enrichment occurring in the upper montane (+0.8‰). Isotopic inputs associated with net precipitaton account for phase, lapse rate and canopy evaporation. Basin-wide, seasonality introduces the greatest spread in isotopic composition with winter months containing the lightest precipitation (−19.8 ± 1.2‰) while summer rain is much heavier (−5.4 ± 1.7‰). With respect to phase, at 0°C and average wind speed, rain is 4.4‰ heavier than snow (refer to Carroll et al., 2022). Elevation produces a 2.9‰ variation in precipitation $\delta^{18}O$ across the ER based on the observed lapse rate. Canopy interception loss accounts for a significant water loss back to the atmosphere (14 ± 5% snowfall). The modeled effect produces lighter net precipitation compared to incoming precipitation. Annually the bias of canopy loss on isotopic influx to the soil is −0.6‰. Modeled results are contradictory to previous research that suggests canopy exchange enriches underlying snowpack (e.g., Koeniger et al., 2008). An explanation of model discrepancy is provided in the discussion.

The calibrated effects of melt and evaporative fractionation on snowpack $\delta^{18}O$ are relatively small compared to literature (O'Neil, 1977), with the calibrated maximum isotopic exchange between liquid water and ice equal to 0.05‰, and ice and vapor equal to 2.1‰. The combined effect of both fractionation process on snowmelt is generally less than 25% total enrichment. In contrast, snowmelt $\delta^{18}O$ evolution is found universally dependent

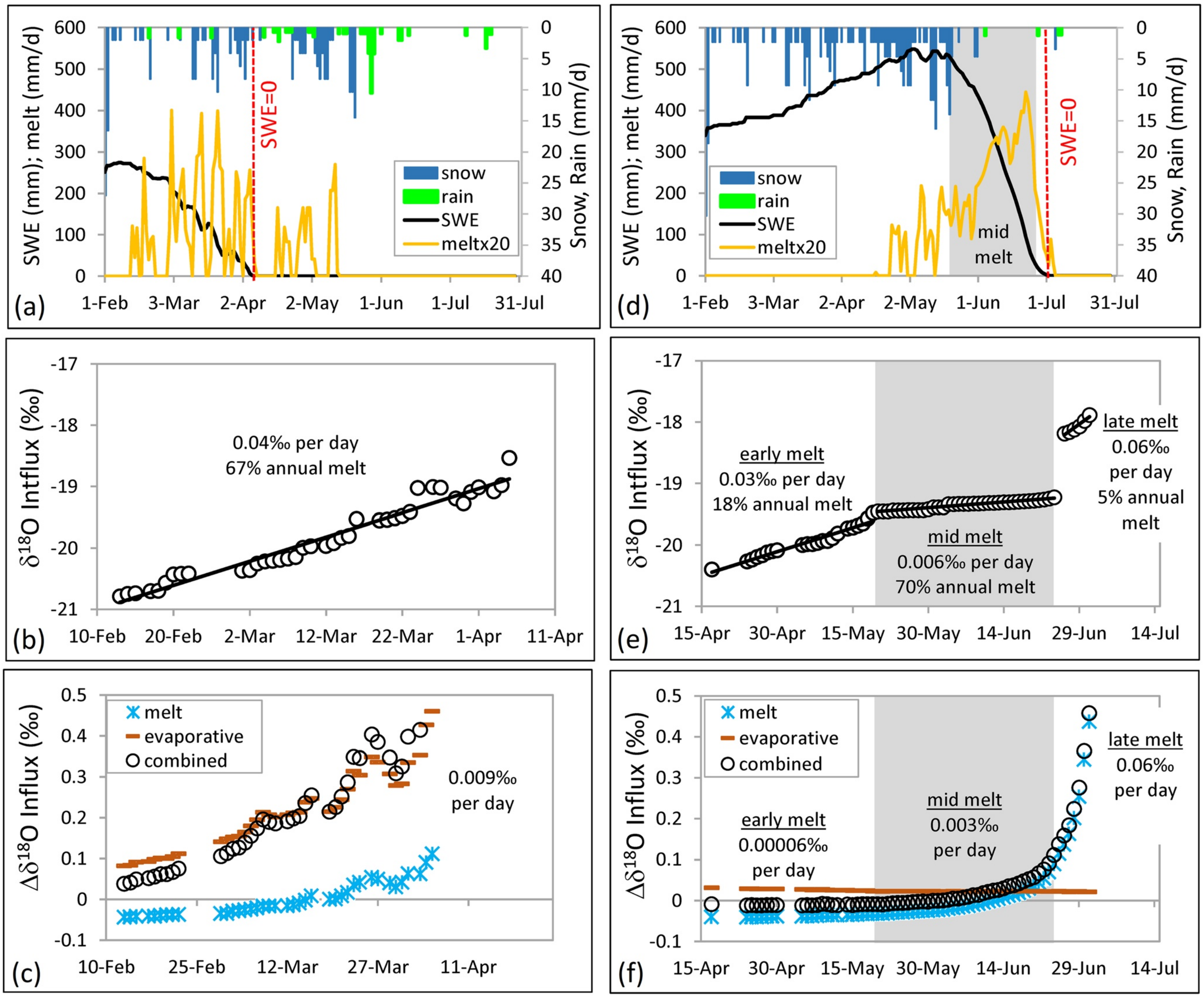

Figure 2. Daily values during an average winter (water year 2016) for a montane meadow (elevation 2,620 m): (a) snow, rain, snowmelt and snow water equivalent, SWE, (b) influx $\delta^{18}O$ during snowmelt of persistent snowpack with enrichment rates provided, (c) effect of melt, evaporative and combined fractionation on $\delta^{18}O$ influx. Daily values for an upper subalpine forest (elevation 3,361 m): (d) snow, rain, snowmelt and SWE, (e) influx $\delta^{18}O$ during snowmelt of persistent snowpack with enrichment rates provided, (f) effect of melt, evaporative and combined fractionation on $\delta^{18}O$ influx. Gray shading for high elevation site identifies melt periods (early, mid, late) as defined by changes in snowmelt enrichment rates.

on elevational effects associated with snow accumulation, the precipitation isotopic lapse rate, and the timing and phase of precipitation during the melt period. To illustrate, the evolution of $\delta^{18}O$ water influx is provided for two locations (Figure 2). The lower elevation site is in a montane meadow (2,620 m). Snowmelt begins on 13 February and enriches by 2.3‰ by early March. Persistent snowpack loss accounts for 67% of the annual snowmelt. Ephermerial snowpack represents the remaining 33% of annual snow water inputs. Snowmelt enrichment is consistent at 0.04‰ per day ($r^2 = 0.95$, $p < 0.01$). The combined effects of melt and evaporative fractionation are +0.6‰, largely through evaporative losses, and represents 25% of the total enrichment over the melt period. Melt enrichment initially depletes snowmelt but accounts for +0.1‰ over time. Spring snowfall and rain are more enriched than the existing snowpack developed over the winter months and account for the bulk of snowmelt enrichment over time. Once SWE = 0, ephemeral snow $\delta^{18}O$ contributions are variable based on seasonal temperature and precipitation phase. The higher elevation site is in a conifer forest in the upper subalpine with a north aspect (3,361 m). Model results suggest this site experiences deep and persistent snowpack with snowmelt delayed until late-April and lasting into early July. Persistent snowpack accounts for 91% of annual snowmelt

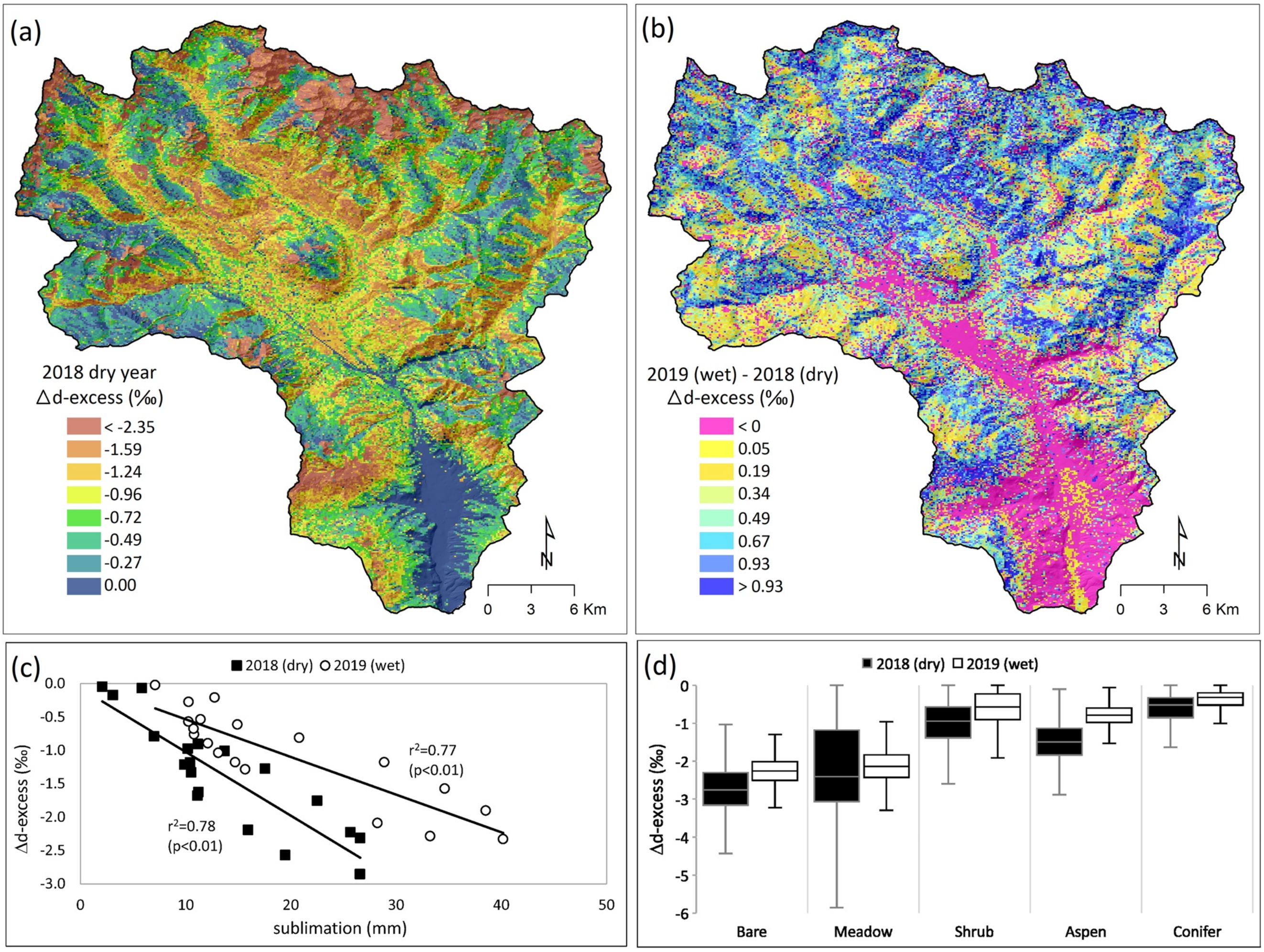

Figure 3. (a) Spatial distribution of snowpack changes to d-excess (Δd-excess) due to post-depostional fractionation during 2018, a dry water year. More negative values indicate greater snowpack fractionation. (c) The difference in Δd-excess between 2019 (wet) and 2018 (dry). Positive values indicate a decrease in fractionation in 2019. (c) Δd-excess as a function of sublimation across elevation aggregated at 50 m increments, (d) Δd-excess for various vegetation cover types.

with little ephemerial snowpack at this site. There are three distinctive melt periods based on enrichment rate and fractionation pocesses. Early melt occurs prior to peak SWE with evaporative and melt fractionation offsetting one another. Instead, the enrichment rate reflects isotopically heavier spring precipitation additions. Mid melt occurs during June and represents the bulk of snow water inputs. Little precipitation adds to the snowpack and snowmelt enrichment is low. With conifer forest shading, evaporative fractionation is also low (+0.02‰). The late melt period is initiated by a rain event contributing to a shallow snowpack at the end of June causing a large jump in $\delta^{18}O$ influx (+1.2‰). Afterwhich, snowmelt enrichment is dominated by melt fractionation (+0.4‰). Fractionation describes 19% the total enrichment with the majority of fractionation applicable to only 5% of the total snowmelt volume.

Simulated kinetic fractionation in bulk snowpack is tracked by decreases in d-excess in snowmelt (Δd-excess) compared to its initial state, or incoming net precipititation. The spatial distribution of Δd-excess is explored using a comparison between a wet/cool (2019) and a dry/warm (2018) water year (Figure 3). In 2018, fractionation is largest in both the barren alpine and the lower subalpine where meadows and aspen forests exist. It is smallest in the conifer forests of the upper subalpine and in the water-limited lower montane that is shrub-dominated. In comparison, 2019, Δd-excess is less negative than 2018 across all ecozones except the lower montane. Snowpack fractionation becomes more influential with increased sublimation but dry water years experience more fractionation for a given amount of sublimation than wet water years (Figure 3c). Basin-wide, daily sublimation losses for 2018 and 2019 are similar for both winters based on energy-limited conditions until late April when sublimation losses in 2019 exceed those in 2018 as a function of snow persistence. By years-end, sublimation loss in 2019 is 23% larger than 2018 but the ratio of sublimation to total snowfall is half (Figure S2 in Supporting Information S1). As a consequence, a more universal, interannual predictor of snowpack fractionation across much of the basin is the ratio of sublimation to snowfall (Figure S3 in Supporting Information S1).

4. Discussion

Similar to previous studies, simulated annual $\delta^{18}O$ water inputs are largely described by the isotopic composition of precipitation (Dahlke & Lyon, 2013; Stichler et al., 1981). The implications of fractionation on $\delta^{18}O$ inputs are found less important in comparison to large seasonal isotopic swings related to air temperature, altitude (Clark & Fritz, 1997; Dansgaard, 164; Otte et al., 2017), as well as the amount, timing and phase of precipitaton. The largest volumes of snowmelt occur in the upper subalpine, where deep and persistent snowpack accumulates over the cold winter months to produce a large pulse of the most depleted water entering the basin. While the isotope model does not account for wind-induced effects on sublimation through saltation (Essery et al., 1999; Wang et al., 2019) or pressure pumping (Colbeck, 1989), wind effects on snow distribution are implicitly accounted for with LiDAR data. In the high alpine, wind moves snow into the upper subalpine. The diminished snowpack in the alpine is combined with large quantities of enriched summer rain from orographically-driven monsoon events to reduce the annual snow fraction and promote heavier isotopic inputs annually compared to the conifer regions. Isotopically heavier water inputs also occur in the montane. This is a combination of the $\delta^{18}O$ lapse rate and temperature-driven phase shifts producing more rain in the fall and spring. Quantifying the isotopic lapse rate, the amount of precipitation and where and when precipitation is rain or snow are critically important to estimating the annual mass flux of $\delta^{18}O$ into the terrestrial system.

The spatial distribution of $\delta^{18}O$ is also dependent on canopy interception. However, the effect is simulated contradictory to other studies. To explain, studies focused on canopy intercepted snow in the intermountain western US indicate $\delta^{18}O$ enrichment of stored snow is approximately 2.1‰ with rates of enrichment increasing for smaller snow particles, denser canopy, longer residence times and under clear-sky conditions (Claassen & Downey, 1995; Koeniger et al., 2008). Exchange of enriched snow from the canopy to the ground can influence isotopic water inputs to the soil. For example, von Freyberg et al. (2019) observed increases in snowpack $\delta^{18}O$ below forest canopy on the order of 2.3‰. Ala-aho et al. (2017) simulated 0.7‰ enrichment in $\delta^{18}O$ in ground snowpack with a three-fold increase in leaf-area index. We find canopy sublimation is consequential and falls within the range of estimates for forested catchments (Mahat & Tarboton, 2014; Pomeroy et al., 1999; Sexstone et al., 2018). While the net effect of canopy loss is appropriate for water balance estimates, PRMS does not allow for exchange of snow in the canopy with the underlying snowpack. It can only be lost back to the atmosphere. The effect is to bias net precipitation (throughfall) toward periods of low PET (deep winter) when canopy storage is not depleted by large evaporative fluxes. The consequence is to shift annual totals of net precipitation toward more depleted isotopic values. This is a model limitation, with wind unloading and canopy melt estimated at >80% of intercepted snowfall in forested regions of northern Utah (Mahat & Tarboton, 2014) and likely an important mechanism of exchange in the ER. Failure to emulate this mechanism likely introduces isotopic mass balance error in the snowpack. Future work will need to explore the effects of canopy interception on water and isotopic mass balances on the underlying snowpack across different forest structures and add capacity to the modeling framework to account for canopy exchange.

Model results indicate fractionation within the snowpack is relatively low, though these process can be important locally and at descrete time intervals. Insensitivity to melt fractionation is not unprecedented. Ala-aho et al. (2017) found a similar result for Bogus Creek in Idaho and suggested this may reflect preferential meltwater flow and limited interaction with the bulk snowpack (Evans et al., 2016; Unnikrishna et al., 2002). Fractionation in the shallow snowpack of open areas is more sensitive to evaporative effects, while deep snowpack in forests is more affected by melt fractionation. In both cases, the net response in snowmelt $\delta^{18}O$ enrichmet during post-depositional fractionation is <25% total enrichment. Instead, isotopically heavier spring precipitation coincident with the ablation period is more consequential. Specifically, for the examples provided in Figure 2 and adjusting for evaporative fractionation, initial enrichment rates are relatively consistent at 0.03‰ per day. With no spring precipitation, snowmelt enrichment is largely abated. This occurs where and when snowpack persists into the often dry month of June. In addition, the largest increases in snowmelt $\delta^{18}O$ occur when rain falls on shallow snowpack. For the conifer example provided, rain on snow produces nearly 50% the total snowmelt enrichment at this location. As a consequence, we suggest less focus needs to address the influence of snowpack fractionation on $\delta^{18}O$ in meltwater in mountain basins where enrichment rates are tightly coupled to elevational effects on snow accumulation, the timing of melt and precipitation phase.

The magnitude of Δd-excess delclines in snowpack can guide where and when sublimation is a critical component of the water balance and can potentially be a tracer for additional insight on water sourcing. Sublimation is a balance of energy and snow water availability. Annually, Δd-excess declines are largest when solar radiation is high and snowfall is low to match trends in the observed snowpit data (Carroll et al., 2022). The winters in the ER are energy-limited and vapor losses from snowpack are estimated relatively small. While increased sublimation may occur in a big snow year due to increased snow persistence, it is not globally sufficient to compensate for large increases in SWE, and snowpack reductions in d-excess that are aggregated in snowmelt are smaller across most of the watershed. Spatially, model results find Δd-excess is highly dependent on vegetation type. The effects of vapor loss is estimated very low in the deep snowpack and conifer forests of the subalpine across all climate conditions. Conifer forests greatly reduce wind scour (Elder et al., 1991) to promote deeper snowpack. Conifer forests also reduce solar radiation on the snowpack surface to limit evaporative losses (Molotch et al., 2009; Musselman et al., 2008; Varhola et al., 2010). Snow water-limitation in the lower montane also reduces the potential for vapor losses, except on wet and cool years when snow availability is sufficient to increase the effect on Δd-excess. Model results suggest the largest vapor losses occur in the barren alpine environment but are likely underestimated because wind effects on sublimation and associated impacts on d-excess are not accounted for in the modeling approach. While error of excluding this mechanism on d-excess modifications in the snowpack is likely large, there is little/no isotopic data at these very high elevations in the ER to confirm. However, current work in the ER is explicitly focused on sublimation mechanisms and future research will incorporate these findings into our modeling framework. Results also indicate sufficient vapor loss in meadows, and desiduous aspen forests during dry water years, to impose on the snowmelt signature. This is done by maximizing the ratio of sublimation to snow water with the largest enrichment occurring in the upper montane. Overall, d-excess offers a comprehensive look at vapor losses for insights on both water balance and water sourcing in the alpine and upper montane environments, and fractionation should be considered for detailed analyses in these portions of the basin. In contrast, post-depositional metamorphism can largely be ignored in the upper subalpine conifer forests where the bulk of snow water enters the system.

5. Conclusions

We combine a hydrologic and snowpack isotopic model to explore the relative importance of landscape position and climate on the spatial and temporal controls of isotopic influxes. The models are calibrated to multiple years of hydrologic and isotopic data. The approach accounts for snow storage, snowmelt timing, rain-on-snow and post-depositional fractionation processes at the scales important to snow dynamics in topographically complex basins. Influxes of $\delta^{18}O$ from snowmelt and rain are dominated by the seasonal variability in precipitation amount, phase and isotopic value with the most depleted inputs occurring in the upper subalpine where snow accumulation is highest and rain inputs minimal. Total enrichment and rate of enrichment in $\delta^{18}O$ meltwater is largely dependent on seasonally enriching springtime precipitation coincident with the snowmelt period as well as rain events on shallow snowpack. In contrast, post-depositional fractionation describes less than 25% meltwater enrichment, though fractionation can be more significant at the local scale and during discreate time periods. As an example, kinetic fractionation by vapor loss, as expressed as decreases in d-excess within the snowpack compared to precipitation, is found important where and when persistent but low snowpack can sustain sufficient sublimation. It is most important in the barren alpine environment (above treeline) and the meadows and aspen forests of the upper montane. Vapor loss effects on snowmelt is least important in the subalpine where snowpack is deep and is shaded by conifer forests. Given the ER is largely energy-limited, wet water years reduce the effect of snowpack kinetic fractionation across the basin. The exception is in the lower montane where snow-limited conditions are moderated by the added snowfall to increase the effect of vapor losses on d-excess declines.

Data Availability Statement

The hydrologic and snowpack isotope model are described in the Supporting Information S1. Data and model files are available to the public and meet FAIR principles. Hydrologic and isotopic model files are located on the U.S. Department of Energy repository ESS-DIVE (https://data.ess-dive.lbl.gov/datasets/doi:10.15485/1889747).

The pre-processing codes and the isotope mixing model are written in fortran and included with the model files. Isotope data for model calibration are available on ESS-DIVE (https://data.ess-dive.lbl.gov/view/doi:10.15485/1824223). The hydrologic model software and documentation are publically available at https://www.usgs.gov/software/gsflow-coupled-groundwater-and-surface-water-flow-model.

Acknowledgments
Funding from the US Department of Energy, Office of Science under contract DE-AC02-05CH11231 through the Lawrence Berkeley National Laboratory Watershed Function Science Focus Area.

References

Ala-aho, P., Tetzlaff, D., McNamara, J. P., Laudon, H., Kormos, P., & Soulsby, C. (2017). Modeling the isotpic evolution of snowpack and snowmelt: Testing a spatially distributed parsimonious approach. *Water Resources Research*, *53*(7), 5813–5830. https://doi.org/10.1002/2017WR020650
Baba, M. W., Gascoin, S., Kinnard, C., Marchane, A., & Hanich, L. (2019). Effect of digital elevation model resolution on the simulation of the snow cover evolution in the high atlas. *Water Resources Research*, *55*(7), 5360–5378. https://doi.org/10.1029/2018WR023789
Bales, R. C., Molotch, N. P., Painter, T. H., Dettinger, M. D., Rice, R., & Dozier, J. (2006). Mountain hydrology of the western United States. *Water Resources Research*, *42*(8), 1–13. https://doi.org/10.1029/2005WR004387
Bearup, L. a., Maxwell, R. M., Clow, D. W., & Mccray, J. E. (2014). Hydrological effects of forest transpiration loss in bark beetle-impacted watersheds. *Nature Climate Change*, *4*(6), 481–486. https://doi.org/10.1038/NCLIMATE2198
Beria, H., Larsen, J. R., Ceperley, N. C., Michelon, A., Vennemann, T., & Schaefli, B. (2018). Understanding snow hydrological processes through the lens of stable water isotopes. *Wiley Interdisciplinary Reviews: Water*, *5*(6), 1–23. https://doi.org/10.1002/wat2.1311
Berkelhammer, M., Still, C., Ritter, F., Winnick, M., Anderson, L., Carroll, R., et al. (2020). Persistence and plasticity in conifer water-use strategies. *Journal of Geophysical Research: Biogeosciences*, *125*(2), e2018JG004845. https://doi.org/10.1029/2018JG004845
Carroll, R. W. H., Bearup, L. A., Brown, W., Dong, W., Bill, M., & Willlams, K. H. (2018). Factors controlling seasonal groundwater and solute flux from snow-dominated basins. *Hydrological Processes*, *32*(14), 2187–2202. https://doi.org/10.1002/hyp.13151
Carroll, R. W. H., Deems, J., Maxwell, R., Sprenger, M., Brown, W., Newman, A., et al. (2022). Variability in observe stable water isotopes in snowpack across a mountainous watershed in Colorado. *Hydrological Processes*, *36*(8). https://doi.org/10.1002/hyp.14653
Carroll, R. W. H., Deems, J. S., Niswonger, R., Schumer, R., & Williams, K. H. (2019). The importance of interflow to groundwater recharge in a snowmelt-dominated headwater basin. *Geophysical Research Letters*, *46*(11), 5899–5908. https://doi.org/10.1029/2019GL082447
Carroll, R. W. H., Gochis, D., & Williams, K. H. (2020). Efficiency of the summer monsoon in generating streamflow within a snow-dominated headwater basin of the Colorado River. *Geophysical Research Letters*, *47*(23), e2020GL090856. https://doi.org/10.1029/2020GL090856
Claassen, H. C., & Downey, J. S. (1995). A model for deuterium and Oxygen-18 isotope changes during evergreen interception of snowfall. *Water Resources Research*, *31*(3), 601–618. https://doi.org/10.1029/94WR01995
Clark, I. D., & Fritz, P. (1997). *Environmental isotopes in hydrogeology* (p. 311). Lewis Publishing. CRP Press LLC.
Clark, M. P., Hendrikx, J., Slater, A. G., Kavetski, D., Anderson, B., Cullen, N. J., et al. (2011). Representing spatial variability of snow water equivalent in hydrologic and land-surface models: A review. *Water Resources Research*, *47*(7), W07539. https://doi.org/10.1029/2011WR010745
Colbeck, S. C. (1989). Air movement in snow due to windpumping. *Journal of Glaciology*, *35*(120), 209–213. https://doi.org/10.3189/s0022143000004524
Cooper, L. W. (1998). Isotopic fractionation in snow cover. *Isotope Tracers in Catchment Hydrology*, 119–136. https://doi.org/10.1016/b978-0-444-81546-0.50011-2
Cowie, R. M., Knowles, J. F., Dailey, K. R., Williams, M. W., Mills, T. J., & Molotch, N. P. (2017). Sources of streamflow along a headwater catchment elevational gradient. *Journal of Hydrology*, *549*, 163–178. https://doi.org/10.1016/j.jhydrol.2017.03.044
Dahlke, H. E., & Lyon, S. W. (2013). Early melt season snowpack isotopic evolution in the Tarfala valley, northern Sweden. *Annals of Glaciology*, *54*(62), 149–156. https://doi.org/10.3189/2013AoG62A232
Earman, S., Campbell, A. R., Phillips, F. M., & Newman, B. D. (2006). Isotopic exchange between snow and atmospheric water vapor: Estimation of the snowmelt component of groundwater recharge in the southwestern United States. *Journal of Geophysical Research*, *111*(9), 1–18. https://doi.org/10.1029/2005JD006470
Elder, K., Dozier, J., & Michaelsen, J. (1991). Snow accumulation and distribution in an alpine watershed. *Water Resources Research*, *27*(7), 1451–1552. https://doi.org/10.1029/91wr00506
Essery, R., Li, L., & Pomeroy, J. (1999). A distributed model of blowing snow over complex terrain. *Hydrological Processes*, *13*(14), 2423–2438. https://doi.org/10.1002/(SICI)1099-1085(199910)13:14/15<2423::AID-HYP853>3.0.CO;2
Evans, S. L., Flores, A. N., Heilig, A., Kohn, M. J., Marshall, H. P., & McNamara, J. P. (2016). Isotopic evidence for lateral flow and diffusive transport, but not sublimation, in a sloped seasonal snowpack, Idaho, USA. *Geophysical Research Letters*, *43*(7), 3298–3306. https://doi.org/10.1002/2015GL067605
Fang, Z., Carroll, R. W. H., Schumer, R., Harman, C., Wilusz, D., & Williams, K. H. (2019). Streamflow partitioning and transit time distribution in snow-dominated basins as a function of climate. *Journal of Hydrology*, *570*, 726–738. https://doi.org/10.1016/j.jhydrol.2019.01.029
Feng, X., Taylor, S., Renshaw, C. E., & Kirchner, J. W. (2002). Isotopic evolution of snowmelt 1. A physically based one-dimensional model. *Water Resources Research*, *38*(10), 35-1–35-8. https://doi.org/10.1029/2001WR000814
Fiorella, R. P., Poulsen, C. J., & Matheny, A. M. (2018). Seasonal patterns of water cycling in a deep, continental mountain valley inferred from stable water vapor isotopes. *Journal of Geophysical Research: Atmospheres*, *123*(14), 7271–7291. https://doi.org/10.1029/2017JD028093
Foster, L. M., Williams, K. H., & Maxwell, R. M. (2020). Resolution matters when modeling climate change in headwaters of the Colorado River. *Environmental Research Letters*, *15*(10), 104031. https://doi.org/10.1088/1748-9326/aba77f
Friedman, I., Benson, C., Gleason, J. I. M., & Survey, S. G. (1991). Isotopic changes during snow metamorphism oD oD (Vol. *3*).
Friedman, I., Smith, G. I., Gleason, J. D., Warden, A., & Harriss, J. M. (1992). Stable isotope composition of waters in Southeastern California 1. Modern precipitation. *Journal of Geophysical Research*, *97*(D5), 5795–5812. https://doi.org/10.1029/92jd00184
Jasechko, S. (2019). Global isotope hydrogeology—Review. *Review of Geophysics*, *57*(3), 835–965. https://doi.org/10.1029/2018RG000627
Koeniger, P., Hubbart, J. A., Link, T., & Marshall, J. D. (2008). Isotopic variation of snow cover and streamflow in response to changes in canopy strucutre in a snow-dominated mountain catchment. *Hydrological Processes*, *22*(4), 557–566. https://doi.org/10.1002/hyp.6967
Mahat, V., & Tarboton, D. G. (2014). Representation of canopy snow interception, unloading and melt in a parsimonious snowmelt model. *Hydrological Processes*, *28*(26), 6320–6336. https://doi.org/10.1002/hyp.10116
Markstrom, S. L., Regan, R. S., Hay, L. E., Viger, R. J., Webb, R. M. T., Payn, R. A., & LaFontaine, J. H. (2015). PRMS-IV, the precipitation-runoff modeling system, version 4. *U.S. Geological Survey Technical Methods*, *6*(B7), 157. https://doi.org/10.3133/tm6B7
Molotch, N. P., Brooks, P. D., Burns, S. P., Litvak, M., Monson, R. K., McConnell, J. R., & Musselman, K. (2009). Ecohydrological controls on snowmelt partitioning in mixed-conifer sub-alpine forests. *Ecohydrology*, *2*, 129–142. https://doi.org/10.1002/eco.48

Mott, R., Vionnet, V., & Grünewald, T. (2018). The seasonal snow cover dynamics: Review on wind-driven coupling processes. *Frontiers of Earth Science*, *6*. https://doi.org/10.3389/feart.2018.00197

Musselman, K. N., Molotch, N. P., & Brooks, P. D. (2008). Effects of vegetation on snow accumulation and ablation in a mid-latitude sub-alpine forest. *Hydrological Processes*, *22*(15), 2767–2776. https://doi.org/10.1002/hyp.7050

Oiro, S., Comte, J. C., Soulsby, C., & Walraevens, K. (2018). Using stable water isotopes to identify spatio-temporal controls on groundwater recharge in two contrasting East African aquifer systems. *Hydrological Sciences Journal*, *63*(6), 862–877. https://doi.org/10.1080/02626667.2018.1459625

O'Neil, J. R. (1977). Stable isotopes in mineralogy. *Physics and Chemistry of Minerals*, *2*(1), 105–123. https://doi.org/10.1007/BF00307527

Otte, I., Detsch, F., Gütlein, A., Scholl, M., Kiese, R., Appelhans, T., & Nauss, T. (2017). Seasonality of stable isotope composition of atmospheric water input at the southern slopes of Mt. Kilimanjaro, Tanzania. *Hydrological Processes*, *31*(22), 3932–3947. https://doi.org/10.1002/hyp.11311

Painter, T. H., Berisford, D. F., Boardman, J. W., Bormann, K. J., Deems, J. S., Gehrke, F., et al. (2016). The airborne snow observatory: Fusion of scanning Lidar, imaging spectrometer, and physically-based modeling for mapping snow water equivalent and snow albedo. *Remote Sensing of Environment*, *184*, 139–152. https://doi.org/10.1016/j.rse.2016.06.018

Pomeroy, J. W., Parviainen, J., Hedstrom, N., & Gray, D. M. (1999). Coupled modelling of forest snow interception and sublimation. *Hydrological Processes*, *12*(15), 2317–2337. https://doi.org/10.1002/(sici)1099-1085(199812)12:15<2317::aid-hyp799>3.0.co;2-x

Sexstone, G. A., Clow, D. W., Fassnacht, S. R., Liston, G. E., Hiemstra, C. A., Knowles, J. F., & Penn, C. A. (2018). Snow sublimation in mountain environments and its sensitivity to forest disturbance and climate warming. *Water Resources Research*, *54*(2), 1191–1211. https://doi.org/10.1002/2017WR021172

Sinclair, K. E., & Marshall, S. J. (2008). Post-depositional modification of stable water isotops in winter snowpacks in the Canadian Rocky Mountains. *Annals of Glaciology*, *49*, 96–106. https://doi.org/10.3189/172756408787814979

Sprenger, M., Leistert, H., Gimbel, K., & Weiler, M. (2016). Illuminating hydrological processes at the soil-vegetation-atmosphere interface with water stable isotopes. *Review of Geophysics*, *54*(3), 674–704. https://doi.org/10.1002/2015RG000515

Stichler, W., Rauert, W., & Martinec, J. (1981). Environmental isotope studies of an alpine snowpack (Weissfluhsoch Switzerland). *Nordic Hydrology*, *12*(4), 297–308. https://doi.org/10.2166/nh.1981.0024

Tappa, D. J., Kohn, M. J., McNamara, J. P., Benner, S. G., & Flores, A. N. (2016). Isotopic composition of precipitation in a topographically steep, seasonally snow-dominated watershed and implications of variations from the global meteoric water line. *Hydrological Processes*, *30*(24), 4582–4592. https://doi.org/10.1002/hyp.10940

Taylor, S., Feng, X., Kirchner, J. W., Osterhuber, R., Klaue, B., & Renshaw, C. E. (2001). Isotopic evolution of a seasonal snowpack and its melt. *Water Resources Research*, *37*(3), 759–769. https://doi.org/10.1029/2000WR900341

Taylor, S., Feng, X., Renshaw, C. E., & Kirchner, J. W. (2002). Isotopic evolution of snowmelt 2. Verification and parameterization of a one-dimensional model using laboratory experiments. *Water Resources Research*, *38*(10), 36-1–36-8. https://doi.org/10.1029/2001wr000815

Taylor, S., Feng, X., Williams, M., & McNamara, J. (2002). How isotopic fractionation of snowmelt affects hydrograph separation. *Hydrological Processes*, *16*(18), 3683–3690. https://doi.org/10.1002/hyp.1232

Unnikrishna, P. V., McDonnell, J. J., & Kendall, C. (2002). Isotope variations in a Sierra Nevada snowpack and their relation to meltwater. *Journal of Hydrology*, *260*(1), 38–57. https://doi.org/10.1016/S0022-1694(01)00596-0

Varhola, A., Coops, N. C., Weiler, M., & Moore, R. D. (2010). Forest canopy effects on snow accumulation and ablation: An integrative review of empirical results. *Journal of Hydrology*, *392* (3), 219–233. https://doi.org/10.1016/j.jhydrol.2010.08.009

von Freyberg, J., Bjarnadottir, T. R., & Allen, S. T. (2019). Influences of forest canopy on snowpack accumulation and isotope ratios. *Journal of Hydrology*, *34*(3), 679–690. https://doi.org/10.1002/hyp.13617

Wang, Z., Huang, N., & Pähtz, T. (2019). The effect of turbulence on drifting snow sublimation. *Geophysical Research Letters*, *46*(20), 11568–11575. https://doi.org/10.1029/2019GL083636

Zhang, Q., Knowles, J. F., Barnes, R. T., Cowier, R. M., Rock, N., & Williams, M. W. (2018). Surface and subsurface water contributions to streamflow from a mesoscale watershed in complex mountain terrain. *Hydrological Processes*, *32*(7), 954–967. https://doi.org/10.1002/hyp.11469